

Ballistic and diffusive: theory of vortices in the two-band superconductor MgB₂

K. Tanaka^{1,2}, D. F. Agterberg^{1,3}, J. Kopu^{4,5}, and M. Eschrig⁵

¹Argonne National Laboratory, Argonne, IL 60439, U.S.A.

²Department of Physics and Engineering Physics,
University of Saskatchewan, Saskatoon, SK, Canada S7N 5E2

³Department of Physics, University of Wisconsin - Milwaukee, P.O. Box 413, Milwaukee, WI 53211, U.S.A

⁴Low Temperature Laboratory, Helsinki University of Technology, PO Box 2200, FIN-02015 HUT, Finland

⁵Institut für Theoretische Festkörperphysik, Universität Karlsruhe, 76128 Karlsruhe, Germany

(Dated: December 6, 2005)

Motivated by the recent results on impurity effects in MgB₂, we present a theoretical model for a two-band superconductor in which the character of quasiparticle motion is ballistic in one band and diffusive in the other. We apply our model to calculate the electronic structure in the vicinity of an isolated vortex. We assume that superconductivity in the diffusive (π) band is induced by that in the clean (σ) band, as suggested by experimental evidence for MgB₂. We focus our attention to the spatial variations of the order parameter, the current density, and the vortex core spectrum in the two bands. Our results indicate that the coupling to the π band can lead to the appearance of additional bound states near the gap edge in the σ band that are absent in the single-band case.

PACS numbers: 74.20.-z, 74.50.+r, 74.70.Ad, 74.81.-g

It is now well established that MgB₂ is a two-gap superconductor, and its essential superconducting properties are well described by an isotropic s -wave two-band model [1, 2, 3, 4, 5, 6, 7]. The two ‘bands’ in MgB₂ are the ‘strong’ σ band that arises from the boron σ -orbitals (with the energy gap $\Delta_\sigma \approx 7.2\text{meV}$), and the ‘weak’ π band that derives from the boron π orbitals ($\Delta_\pi \approx 2.3\text{meV}$). Despite the fact that each ‘band’ consists in reality of a pair of bands, the variation of the gap within each corresponding pair of Fermi-surface sheets can be neglected [8, 9]. The two energy gaps are observed to vanish at a common transition temperature T_c : no second transition has been observed, and there is evidence of induced superconductivity in the π band [5, 10, 11].

There have been considerable efforts to understand impurity effects in MgB₂ [7]. Besides the potential applications of MgB₂ as magnetic devices [12], these studies have aimed at testing a prediction of the two-band model: the reduction of T_c and the gap ratio by non-magnetic impurities. However, Mazin *et al.* [13, 14] have shown that this does not apply to MgB₂, i.e. to Mg-site impurities or defects, which are more favourable energetically than those at B sites. While the π band is strongly affected by such impurities, the σ band is more robust, and there is little mixing of the two bands because of negligible interband scattering [13, 14]. This is consistent with accumulating experimental evidence suggesting that the σ and π bands are essentially in the ballistic and diffusive limit, respectively [15] (see also references in Refs. [13, 14]). Nevertheless, so far in theoretical studies both of the two bands have been assumed to be either in the clean [16] or in the dirty limit [17].

In this Letter, we examine theoretically the effects of induced superconductivity and impurities on the vortex-core structure in a two-band superconductor. Our work is motivated by the experimental investigation of the vor-

tex state in MgB₂ using scanning tunnelling spectroscopy [10]. We present a novel formulation of coupled quasiclassical Eilenberger and Usadel equations to describe a multiband superconductor with one ballistic and one diffusive band with negligible interband scattering: the two bands are assumed to be coupled only by the pairing interaction.

We apply our model to calculate numerically the local density of states (LDOS) and supercurrent density around an isolated vortex. We examine in detail the intriguing spatial variation of these quantities and the order parameter in the two bands. A particularly interesting result emerging from our studies is the possibility of additional bound states near the gap edge in the σ band.

Our model is based on the equilibrium quasiclassical theory of superconductivity, where the physical information is contained in the Green function, or propagator, $\hat{g}(\epsilon, \mathbf{p}_{F\alpha}, \mathbf{R})$. Here ϵ is the quasiparticle energy measured from the chemical potential, $\mathbf{p}_{F\alpha}$ the quasiparticle momentum on the Fermi surface of band $\alpha \in \{\sigma, \pi\}$, and \mathbf{R} is the spatial coordinate (the hat refers to the 2×2 matrix structure of the propagator in the particle-hole space). In the clean σ band, $\hat{g}_\sigma(\epsilon, \mathbf{p}_{F\sigma}, \mathbf{R})$ satisfies the Eilenberger equation [18]

$$[\epsilon \hat{\tau}_3 - \hat{\Delta}_\sigma, \hat{g}_\sigma] + i \mathbf{v}_{F\sigma} \cdot \nabla \hat{g}_\sigma = \hat{0}, \quad (1)$$

where $\mathbf{v}_{F\sigma}$ is the Fermi velocity and $\hat{\Delta}_\sigma$ the (spatially varying) order parameter in the σ band. Throughout this work, we ignore the external magnetic field (this is justified because MgB₂ is a strong type-II superconductor). The coherence length in the σ band is defined as $\xi_\sigma = v_{F\sigma}/2\pi T_c$.

In the presence of strong impurity scattering, the Green function has no momentum dependence and the Eilenberger equation reduces to the Usadel equation [19].

We assume this to be the appropriate description for the dirty π band, and take the propagator $\hat{g}_\pi(\epsilon, \mathbf{R})$ to satisfy

$$\left[\epsilon \hat{\tau}_3 - \hat{\Delta}_\pi, \hat{g}_\pi \right] + \frac{D}{\pi} \nabla \cdot (\hat{g}_\pi \nabla \hat{g}_\pi) = \hat{0}. \quad (2)$$

The diffusion constant D defines the π -band coherence length as $\xi_\pi = \sqrt{D/2\pi T_c}$. Additionally, both propagators are normalized according to $\hat{g}_\sigma^2 = \hat{g}_\pi^2 = -\pi^2 \hat{1}$.

We assume that the quasiparticles in different bands are coupled only through the pairing interaction, neglecting interband scattering by the impurities. The gap equations for the multiband system are given as

$$\Delta_\alpha(\mathbf{R}) = \sum_\beta V_{\alpha\beta} N_{F\beta} \mathcal{F}_\beta(\mathbf{R}), \quad (3)$$

where $\alpha, \beta \in \{\sigma, \pi\}$, $\hat{\Delta}_\alpha = \hat{\tau}_1 \text{Re } \Delta_\alpha - \hat{\tau}_2 \text{Im } \Delta_\alpha$, the coupling matrix $V_{\alpha\beta}$ determines the strength of the pairing interaction, $N_{F\beta}$ is the Fermi-surface density of states on band β , and

$$\begin{aligned} \mathcal{F}_\sigma(\mathbf{R}) &\equiv \int_{-\epsilon_c}^{\epsilon_c} \frac{d\epsilon}{2\pi i} \langle f_\sigma(\epsilon, \mathbf{p}_{F\sigma}, \mathbf{R}) \rangle_{\mathbf{p}_{F\sigma}} \tanh\left(\frac{\epsilon}{2T}\right), \\ \mathcal{F}_\pi(\mathbf{R}) &\equiv \int_{-\epsilon_c}^{\epsilon_c} \frac{d\epsilon}{2\pi i} f_\pi(\epsilon, \mathbf{R}) \tanh\left(\frac{\epsilon}{2T}\right). \end{aligned} \quad (4)$$

Here f_α is the upper off-diagonal (1,2) element of the matrix propagator \hat{g}_α , $\langle \dots \rangle_{\mathbf{p}_{F\sigma}}$ denotes averaging over the σ band Fermi surface, and ϵ_c is a cut-off energy.

We solve the system of equations (1)–(4) numerically. The normalization condition is taken into account with the Riccati parameterisation for the Green functions [20, 21]. After self-consistency has been achieved for the order parameter, the (for the σ band angle-resolved) LDOS in each band can be calculated as

$$\begin{aligned} N_\sigma(\epsilon, \mathbf{p}_{F\sigma}, \mathbf{R})/N_{F\sigma} &= -\text{Im } g_\sigma(\epsilon, \mathbf{p}_{F\sigma}, \mathbf{R})/\pi, \\ N_\pi(\epsilon, \mathbf{R})/N_{F\pi} &= -\text{Im } g_\pi(\epsilon, \mathbf{R})/\pi, \end{aligned} \quad (5)$$

where g_α is the upper diagonal (1,1) element of \hat{g}_α .

The current density around the vortex has contributions from both the π band and the σ band. The corresponding expressions are ($e = -|e|$ is the electron charge)

$$\begin{aligned} \frac{\mathbf{j}_\sigma(\mathbf{R})}{2eN_{F\sigma}} &= \int_{-\infty}^{\infty} \frac{d\epsilon}{2\pi} \langle \mathbf{v}_{F\sigma} \text{Im } g_\sigma \rangle_{\mathbf{p}_{F\sigma}} \tanh\left(\frac{\epsilon}{2T}\right), \\ \frac{\mathbf{j}_\pi(\mathbf{R})}{2eN_{F\pi}} &= \frac{D}{\pi} \int_{-\infty}^{\infty} \frac{d\epsilon}{2\pi} \text{Im } [f_\pi^* \nabla f_\pi] \tanh\left(\frac{\epsilon}{2T}\right). \end{aligned} \quad (6)$$

Throughout this work, we focus on the effects of purely induced superconductivity in the π band. Diagonalization of the coupling matrix in Eq. (3) decouples the gap equations. The larger of the two eigenvalues of the matrix $V_{\alpha\beta} N_{F\beta}$, denoted by $\lambda^{(0)}$, determines the critical temperature T_c and can be eliminated together with ϵ_c . The

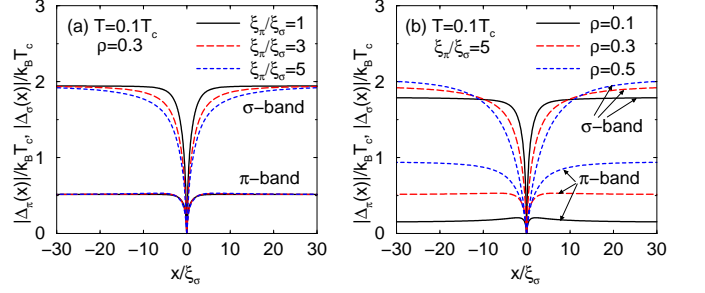


FIG. 1: Magnitude of the order parameter, $|\Delta_{\sigma,\pi}(x)|$, in the σ - and π band, as a function of coordinate x on a path through the vortex center, at $T = 0.1T_c$: (a) for different ratios ξ_π/ξ_σ and fixed strength of the induced π -band gap, parameterized by the mixing ratio (see text), $\rho = 0.3$; (b) for different ρ and fixed $\xi_\pi/\xi_\sigma = 5$. A weak effective repulsion due to Coulomb interaction was assumed in the subdominant $\lambda^{(1)}$ pairing channel, parameterized by $\Lambda = -0.1$ (see text).

smaller eigenvalue $\lambda^{(1)}$ is parameterized by the cut-off independent combination $\Lambda = \lambda^{(0)}\lambda^{(1)}/(\lambda^{(0)} - \lambda^{(1)})$. The pairing interactions have been calculated with ab initio methods, employing an electron-phonon coupling model [3, 8]; from these studies, taking Coulomb repulsion into account [9], we estimate $\Lambda < 0.3$ for MgB₂. We present results for $\Lambda = -0.1$ (implying a weak repulsion in the subdominant $\lambda^{(1)}$ channel). The ratio of the magnitude of the bulk gaps $\rho = |\Delta_\pi^{\text{bulk}}|/|\Delta_\sigma^{\text{bulk}}|$ near T_c parameterizes the strength of the induced superconductivity in the π band; experimentally $\rho \approx 0.3$ in MgB₂. For simplicity, we have set $N_{F\sigma} = N_{F\pi}$ in our calculations; the densities of states of the two bands are indeed of comparable size [8, 9]. A cylindrical Fermi surface was used for the two-dimensional σ band. For the ratio of the coherence lengths in the two bands we present results for $\xi_\pi/\xi_\sigma = 1, 3$, and 5. An estimate from experiments [10, 22] gives for MgB₂ a value between 1 and 3.

In Fig. 1 we present the order-parameter magnitudes for each band as a function of coordinate x along a path through the vortex center. In Fig. 1 (a) we show the order parameter variation at $T = 0.1T_c$ for several coherence-length ratios ξ_π/ξ_σ and gap ratio $\rho = 0.3$. Surprisingly, we find that an increase of ξ_π results in an increase of the recovery length of the order parameter (the characteristic length over which the order parameter changes from zero to the bulk value) in the σ band, while the recovery length in the π band is barely affected. Thus, the recovery lengths in the two bands can differ considerably, even though the superconductivity in the π band is induced by the σ band. In Fig. 1 (b), the gap ratio ρ is varied for fixed $\xi_\pi/\xi_\sigma = 5$. One can see that, apart from the well-known increase of the bulk Δ_σ/T_c ratio with increasing bulk Δ_π , the recovery length in the σ band increases considerably with increasing ρ . The π -band recovery length is also enhanced together with that of the σ band if $\rho > 0.3$, as clearly seen for $\rho = 0.5$. For

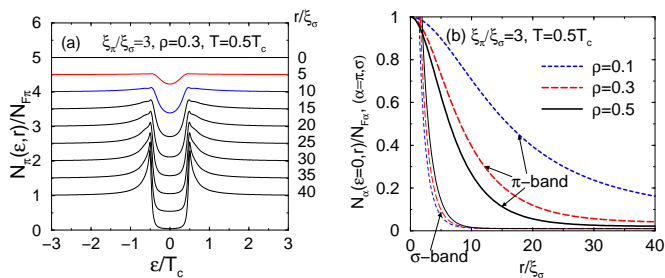


FIG. 2: (a) Local density of states (LDOS) for the π band, as a function of energy ϵ for different distances r from the vortex center. The spectra are shifted in vertical direction for convenience. (b) LDOS at the chemical potential, $\epsilon = 0$, as a function of r for different ρ and fixed $T = 0.5T_c$, $\xi_\pi/\xi_\sigma = 3$.

$\rho = 0.1$, Δ_π near the vortex core is enhanced from its bulk value.

To understand these effects we have performed calculations for different values of Λ that characterizes the Coulomb repulsion in the π band. We have found that for $\Lambda > 0$ the ratio $|\Delta_\pi|/|\Delta_\sigma|$ is reduced in the core region with respect to its bulk value, however is enhanced for $\Lambda < 0$. This leads to a renormalization of the recovery lengths of the order parameters in both bands.

In Fig. 2 we show the spectral properties of the π band. The LDOS, shown in Fig. 2 (a), is flat at the vortex center ($r = 0$), in agreement with the experiment of Ref. [10]. Outside the vortex core the BCS density of states is recovered. The decay of the zero-bias LDOS as a function of radial coordinate is shown in Fig. 2 (b), and compared with that of the σ band [obtained from the data in Fig. 3 (a)]. The decay length of the zero-bias DOS is clearly different for the two bands. For the π band it is given by $\xi_\pi \sqrt{\Delta_\sigma/\Delta_\pi}$, and thus dominated by the parameter ρ . In the σ band the length scale of the decay is ξ_σ , and thus shorter than that in the π band. The existence of two apparent length scales in the LDOS was also reported in the case of two clean bands [16] and two dirty bands [17].

In Fig. 3 we show the vortex-core spectra in the σ band. The LDOS, $N_\sigma(\epsilon, \mathbf{R}) = \langle N_\sigma(\epsilon, \mathbf{p}_{F\sigma}, \mathbf{R}) \rangle_{\mathbf{p}_{F\sigma}}$, as a function of energy for different distances from the vortex center is plotted in Fig. 3 (a), showing the well-known Caroli-de Gennes-Matricorn bound-state bands at low energies. The new feature of our model is the additional bound states in the vortex-core region near the gap edges, that are clearly visible in Fig. 3 (a). This is in strong contrast with the case of a single-band superconductor, where the spectrum near the vortex center is suppressed at the gap edges, showing neither a coherence peak nor additional bound states. We note that the self-consistency of the order-parameter profile is essential for discussing the presence of the bound states at the gap edges. We illustrate the development of these additional bound states in terms of the spectrum at the vortex center. We find that for a given ξ_π/ξ_σ , the bound state exists

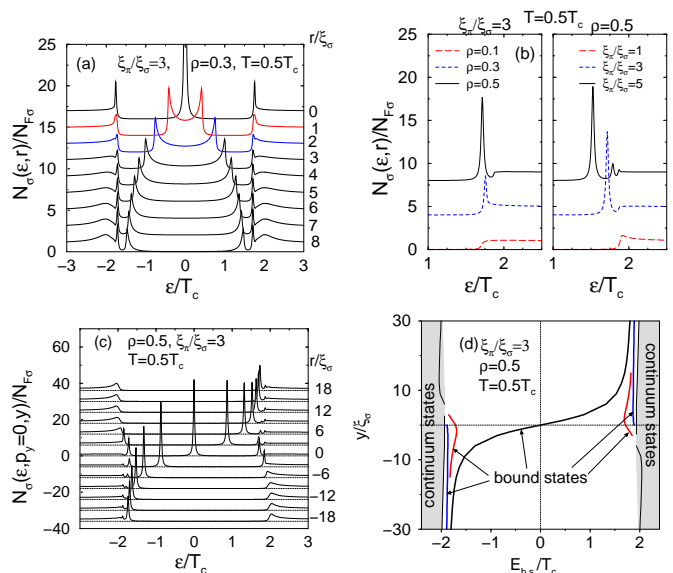


FIG. 3: (a) LDOS for the σ band as a function of energy ϵ for different distances r from the vortex center. (b) The development of an extra bound state near the gap edge in the σ band for different parameter combinations. The bound state develops for sufficiently large mixing ratio ρ and coherence length ratio ξ_π/ξ_σ . (c) Angle-resolved LDOS for quasiparticles with momentum along the x axis in the σ band, showing the bound states as a function of y . The dispersion of the bound states as a function of y is also shown in (d) for $\rho = 0.5$, $\xi_\pi/\xi_\sigma = 3$ and $T = 0.5T_c$. Spectra in (a)-(c) are shifted in vertical direction for convenience.

for ρ larger than a certain critical value, as seen in the left panel of Fig. 3 (b). For a given ρ , on the other hand, the bound state develops if ξ_π/ξ_σ exceeds a critical value, which is between 1 and 3 for $\rho = 0.3$, as can be inferred from the right panel of Fig. 3 (b). The bound states are, e.g., clearly resolved for $\rho = 0.3$ and $\xi_\pi/\xi_\sigma = 3$, values appropriate for MgB_2 . We have found a similar bound state spectrum also for $\Lambda > 0$. The bound states move with the gap edge as a function of temperature.

The bound-state spectrum is most clearly discussed in terms of the angle-resolved spectra, shown in Fig. 3 (c). Here the spectrum of quasiparticles moving in the x direction is shown as a function of position along the y axis. The position of the bound states as a function of y is shown in Fig. 3 (d). The main bound state branch crosses the chemical potential in the vortex center. The additional bound states are seen near the gap edge, and show a weak dispersion. In fact, a close inspection reveals that there are two additional branches; however, only one of them is present at the vortex center.

Finally, in Fig. 4 we show contributions from the two bands to the supercurrent density around the vortex separately. We show the results for $\rho = 0.3$, and (a) $\xi_\pi/\xi_\sigma = 1$, (b) $\xi_\pi/\xi_\sigma = 3$, and (c) $\xi_\pi/\xi_\sigma = 5$, at $T/T_c = 0.1, 0.3$ and 0.5 . The current density from the

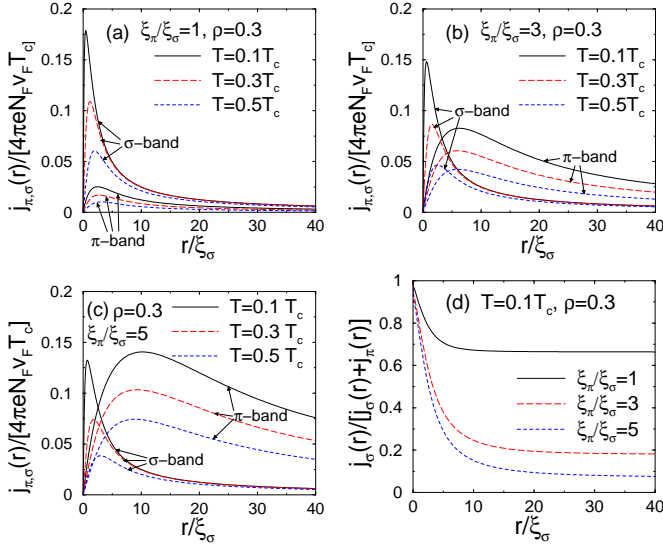


FIG. 4: Contribution to the current density as a function of distance from the vortex center, shown separately for the π band and the σ band for fixed mixing ratio $\rho = 0.3$ and different temperatures T ; (a) for $\xi_\pi/\xi_\sigma = 1$, (b) $\xi_\pi/\xi_\sigma = 3$, and (c) $\xi_\pi/\xi_\sigma = 5$. In (d) the σ -band contribution to the total current density is shown as a function of radial coordinate, for $T = 0.1T_c$, $\rho = 0.3$, and different ξ_π/ξ_σ .

σ band is enhanced for low temperatures near the vortex center, and the maximum approaches the center for $T \rightarrow 0$. This is due to the well-known Kramer-Pesch effect for the clean σ band. The current density due to the induced superconductivity in the π band is also enhanced by decreasing temperature, but the maximum does not approach the vortex center as in the σ band. With increasing r , the contribution of the σ band is reduced, and the contribution of the π band becomes considerable when $\xi_\pi/\xi_\sigma \gtrsim 1$. At the same time, \mathbf{j}_σ shows temperature dependence only in the core area, whereas \mathbf{j}_π is temperature dependent also far outside the core. To discuss this effect, we note that at a large distance r from the vortex center (but small compared to the London penetration depth), the current-density magnitudes are approximately given by $j_\sigma(r) \sim eN_F\sigma v_F^2/2r$ and $j_\pi(r) \sim eN_F\pi\pi D|\Delta_\pi|/r$. The temperature dependence of j_π is thus dominated by that of $|\Delta_\pi|$.

Another important observation is that, for the parameters appropriate for MgB₂, the contribution of j_π is considerable outside the vortex core. In fact, already for a moderate ratio $\xi_\pi/\xi_\sigma = 3$ the σ -band contribution is restricted to the region very close to the vortex center and is negligible outside the core for $\rho \geq 0.3$. To understand this effect, shown in Fig. 4 (d), we note that the current-density ratio far away from the vortex center approaches

$$\lim_{r \gg \xi_{\pi,\sigma}} \frac{j_\pi(r)}{j_\sigma(r)} = \frac{2D\pi|\Delta_\pi|}{v_F^2\sigma} = \frac{|\Delta_\pi|}{T_c} \left(\frac{\xi_\pi}{\xi_\sigma} \right)^2. \quad (7)$$

Clearly, the π -band contribution to the current density

dominates when $(\xi_\pi/\xi_\sigma)^2 > (|\Delta_\pi|/T_c)^{-1}$, which is a case relevant for MgB₂.

In conclusion, we have formulated a model for coupled ballistic and diffusive bands in terms of coupled Eilenberger and Usadel equations. We have studied the effects of induced superconductivity in the ‘weak’ diffusive band on the order parameter, the current density and the spectral properties of the ‘strong’ ballistic band. We have found that (a) the recovery lengths of the order parameters in the two bands are renormalized by Coulomb interactions; (b) the vortex core spectrum in the σ band shows additional bound states at the gap edges; and (c) the current density is dominated in the vortex core by the σ -band contribution, and outside the vortex core the π band contribution is substantial, or even dominating, for parameters appropriate for MgB₂. Our predictions concerning the vortex-core spectrum of the σ band can be tested in future tunnelling experiments.

We acknowledge discussions with B. Jankó, M. Iavarone, M.W. Kwok, and H. Schmidt, and support by the NSERC of Canada, the U.S. DOE, Basic Energy Sciences (W-7405-ENG-36), the NSF (DMR-0381665), and the Deutsche Forschungsgemeinschaft within the CFN.

- [1] J. Nagamatsu *et al.*, Nature (London) **410**, 63 (2001).
- [2] S.V. Shulga *et al.*, cond-mat/0103154 (2001).
- [3] A. Y. Liu, I. I. Mazin, J. Kortus, Phys. Rev. Lett. **87**, 087005 (2001); A. A. Golubov *et al.*, J. Phys.: Condens. Matter **14**, 1353 (2002).
- [4] F. Bouquet, *et al.*, Europhys. Lett. **56**, 856 (2001).
- [5] H. Schmidt *et al.*, Phys. Rev. Lett. **88**, 127002 (2002).
- [6] M. Iavarone *et al.*, Phys. Rev. Lett. **89**, 187002 (2002).
- [7] Special issue on MgB₂, Physica (Amsterdam) **385C**, issues 1-2, (2003); T. Dahm in *Frontiers in Superconducting Materials*, ed. A.V. Narlikar, Springer (2005).
- [8] H. J. Choi *et al.*, Nature (London) **418**, 758 (2002).
- [9] I. I. Mazin *et al.*, Phys. Rev. B **69**, 056501 (2004).
- [10] M. R. Eskildsen *et al.*, Phys. Rev. Lett. **89**, 187003 (2002); Phys. Rev. B **68**, 100508(R) (2003).
- [11] J. Geerk *et al.*, Phys. Rev. Lett. **94**, 227005 (2005).
- [12] A. Gurevich *et al.*, Supercond. Sci. Technol. **17**, 278 (2004).
- [13] I. I. Mazin *et al.*, Phys. Rev. Lett. **89**, 107002 (2002).
- [14] S. C. Erwin, I. I. Mazin, Phys. Rev. B **68**, 132505 (2003).
- [15] M. Putti *et al.*, Phys. Rev. B **67**, 064505 (2003); *ibid.* **70**, 052509 (2004); *ibid.* **71**, 144505 (2005); J. W. Quilty, *et al.*, Phys. Rev. Lett. **90**, 207006 (2003); M. Ortolani *et al.*, Phys. Rev. B **71**, 172508 (2005); A. Carrington *et al.*, Phys. Rev. B **72**, 060507(R) (2005).
- [16] N. Nakai, M. Ichioka, K. Machida, J. Phys. Soc. Japan **71**, 23 (2002).
- [17] A. E. Koshelev, A. A. Golubov, Phys. Rev. Lett. **90**, 177002 (2003).
- [18] G. Eilenberger, Z. Phys. **214**, 195 (1968).
- [19] K. Usadel, Phys. Rev. Lett. **25**, 507 (1970).
- [20] N. Schopohl and K. Maki, Phys. Rev. B **52**, 490 (1995).
- [21] M. Eschrig, Phys. Rev. B **61**, 9061 (2000); M. Eschrig *et al.*, Adv. in Sol. State Phys. **44**, 533, Springer (2004); M. Eschrig *et al.* in *Vortices in Unconventional Superconductors and Superfluids*, eds. R.P. Huebener, N. Schopohl,

- and G.E. Volovik, Springer (2002).
- [22] S. Serventi *et al.*, Phys. Rev. Lett. **93**, 217003 (2004).